Evidence of quinonoid structures in the vibrational spectra of thiophene based conducting polymers: Poly(thiophene), poly (thieno [3,4-b] benzene) , and poly (thieno [3,4-b] pyrazine)

Lilee Cuff and Miklos Kertesz

Citation: The Journal of Chemical Physics **106**, 5541 (1997); doi: 10.1063/1.473576
View online: http://dx.doi.org/10.1063/1.473576
View Table of Contents: http://scitation.aip.org/content/aip/journal/jcp/106/13?ver=pdfcov
Published by the AIP Publishing

Articles you may be interested in

Conductivity enhancement of poly(3,4-ethylenedioxythiophene)-poly(styrenesulfonate) films post-spincasting
J. Appl. Phys. **112**, 113709 (2012); 10.1063/1.4768265

First-principles studies of electronic, optical, and vibrational properties of LaVO 4 polymorph
J. Appl. Phys. **108**, 093519 (2010); 10.1063/1.3499308

Simulations of vibrational spectra from classical trajectories: Calibration with ab initio force fields
J. Chem. Phys. **127**, 084502 (2007); 10.1063/1.2756837

A theoretical anharmonic study of the infrared absorption spectra of F H F − , F D F − , O H F − , and O D F − anions
J. Chem. Phys. **124**, 174308 (2006); 10.1063/1.2191042

Symmetry breaking effects in NO 3 − : Raman spectra of nitrate salts and ab initio resonance Raman spectra of nitrate–water complexes
J. Chem. Phys. **114**, 6249 (2001); 10.1063/1.1355657

This article is copyrighted as indicated in the article. Reuse of AIP content is subject to the terms at: http://scitation.aip.org/termsconditions. Downloaded to IP: 128.114.34.22 On: Fri, 28 Nov 2014 10:08:48

Evidence of quinonoid structures in the vibrational spectra of thiophene based conducting polymers: Poly(thiophene), poly(thieno[3,4-*b*]benzene), and poly(thieno[3,4-*b*]pyrazine)

Lilee Cuff and Miklos Kertesz[a)]
Department of Chemistry, Georgetown University, Washington, DC 20057-1227

(Received 12 January 1996; accepted 20 December 1996)

By combining vibrational spectra and *ab initio* calculations, we obtained a consistent description of the IR and nonresonant Raman spectra, including intensities, of four thiophene based polymers—undoped and heavily doped poly(thiophene) (PTh), undoped poly(thieno[3,4-*b*]benzene) (PITN), and poly(thieno[3,4-*b*]pyrazine) (PThP) for the first time. Predicted spectra for poly(thiophene) agree with experiment very well. Based on the calculated force constants and Badger's rule, we also estimated the average inter-ring bond lengths of undoped and doped PTh to be 1.47 and 1.42 Å, respectively. The latter leads to an estimated 33% quinonoid character on average for heavily doped PTh. The average inter-ring bond lengths of undoped PITN and PThP, that are consistent with their vibrational spectra, are estimated to be 1.41, and 1.42 Å, respectively. These values showed that undoped PITN and PThP have quinonoid character close to that of heavily doped PTh. Further, we also estimated that, upon doping the average bond lengths of PTh changed by -0.01, 0.11, and -0.05 Å for intra-ring C_β–C_β, C_α–C_β, and inter-ring bonds, respectively. These bond length changes are significantly different from those of Hartree–Fock-type calculations, reflecting significant correlation contributions and are also in conflict with earlier empirical fits of the vibrational spectrum of the highly doped phase of PTh. However, our results are more in line with the generally accepted picture of an aromatic to quinonoid ''transition'' of the doping process. Furthermore, the counterintuitive downward frequency shifts in the vibrational spectra of PTh upon doping can be explained by the structural change from an essentially aromatic to a partially quinonoid form. © *1997 American Institute of Physics.* [S0021-9606(97)51612-6]

I. INTRODUCTION

Poly(thiophene) (PTh) has been a favorite in the conducting polymer field, being a prototypical conjugated polymer with a nondegenerate ground state. In addition, PTh is also useful because it has good stability,[1] high conductivity,[2] and large nonlinear optical response.[3] A comprehensive review on synthesis, characterization, and applications of PTh has been published recently by Roncali.[4] Two related polymers, poly(thieno[3,4-*b*]benzene) [also known as poly(isothianaphthene) (PITN)], and poly(thieno[3,4-*b*]pyrazine) (PThP) were recently synthesized by Wudl *et al.*[5] and Pomerantz *et al.*,[6] respectively. These two polymers have low band gaps close to 1.0 eV (Refs. 6–8) and are illustrated in Fig. 1 together with the purely aromatic and purely quinonid forms of PTh.

One major obstacle to the understanding of fundamental properties of conducting polymers is the lack of enough detailed structural data. The present work focuses on extracting structural data from a combination of vibrational spectra taken from the literature and *ab initio* calculations.

In our previous work, we have successfully used theoretical modeling, specifically the scaled quantum mechanical oligomer force field (SQMOFF) method,[9] that produces not only vibrational frequencies that agree well with experimental data, but also IR and Raman intensities that are in reasonable agreement with experiment. The limitations of the SQMOFF method are

(i) An infinite periodic model of the polymer is assumed; which exhibits translational or helical symmetry.
(ii) The calculated Raman intensities are based on Placzek's theory (nonresonant intensities).
(iii) The force fields are based on empirically scaled quantum chemical *ab initio* calculations with a basis set that is usually limited.
(iv) When applied to doped polymers, these calculations introduce further approximations by assuming a uniform doped structure. By ignoring polarons and bipolarons, these vibrational calculations correspond to an average doped polymer structure, and therefore the quality of the agreement with experiment is inferior as compared to the undoped calculations.

We have used similar calculations in conjunction with the experimental Raman spectra to quantitatively estimate the structural changes of poly(*p*-phenylene) (PPP) upon doping.[9(b)] In this paper, we will use this two-pronged approach to examine the structures of three thiophene based heterocyclic conjugated conducting polymers; PTh, PITN, and PThP.

Although the vibrational spectroscopic properties of PTh have been studied before,[10,11] it was not until recently that a Raman spectrum of a heavily doped PTh which exhibited marked downward frequency shifts relative to the undoped

a)Author to whom correspondence should be addressed.

This article is copyrighted as indicated in the article. Reuse of AIP content is subject to the terms at: http://scitation.aip.org/termsconditions. Downloaded to IP: 128.114.34.22 On: Fri, 28 Nov 2014 10:08:48

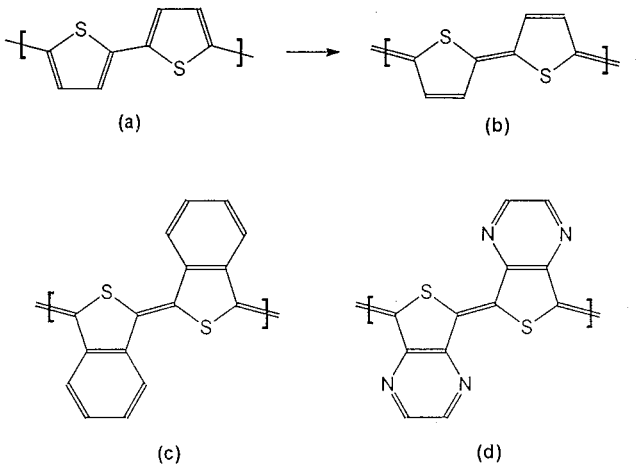

FIG. 1. The repeat unit of (a) undoped PTh, (b) heavily doped PTh, (c) undoped PITN and (d) undoped PThP. Note that undoped PTh is aromaticlike while heavily doped PTh, undoped PITN and PThP are quinonoidlike.

material was reported by Louarn *et al.*,[12] and by Furukawa *et al.*[13] According to oligomer calculations of Bredas *et al.*,[14] the ground state structure of PTh is aromatic, having essentially C–C single bonds between two adjacent rings. They[14] and others[10] also found that the structure of PTh changes to a bipolaronic structure upon doping, thereby attaining a degree of C═C double bond character between rings in the bipolaronic domain [see Fig. 1(b)]. It is therefore counterintuitive that the frequencies of heavily doped PTh, especially those with inter-ring stretching characteristics, should shift towards lower frequencies. One obvious question is, whether the data could be interpreted by assuming a quinonoidlike ground state for PTh. The energy difference between the aromatic and the quinonoid structures of PTh is significant; estimates range (in kcal/mol per ring unit) from 16. (Ref. 14) to 9.6–4.5 (Ref. 7) to 3.5,[15] all indicating that an aromaticlike structure is more stable. Therefore, it is reasonable to conclude that a quinonoid ground state is not likely. In order to understand the observed frequency shifts, we carry out normal mode calculations and are able to provide a plausible explanation to the vibrational frequency shifts while maintaining the fundamental picture of an aromatic to quinonoid ''transition'' upon doping.[14,16]

Theoretical calculations by Lee and Kertesz,[7] Karpfen and Kertesz,[15] Kurti *et al.*,[17] Nayak and Marynick,[18] Kastner *et al.*,[19] and Hoogmartens *et al.*[20] have shown that the ground state of the two thiophene related polymers, PITN and PThP, are quinonoid to some degree. The reversal of stability of the aromaticlike vs the quinonoidlike structures going from PTh to PITN has been shown[7] to be related to the reversal of the HOMO and LUMO levels upon the condensation of a six-membered ring onto each thiophene ring. Estimates[7,15] for the energy difference (in kcal/mol per ring of PITN) range from 3.0 to 11.2, all showing quinonoidlike structures to be more stable than the aromatic ones. Because of higher steric hindrances, quinonoid PITN has a lower net stabilization energy compared to quinonoid PThP.[18] It must be emphasized that these calculated results correspond to infinite chains or extrapolations to infinite chains. Kurti and Surjan[21] have pointed out that due to end effects, there exists a critical chain length for PITN below which the ground state structure is essentially aromatic, assuming that H or another single bonded species are the terminal groups.

Attempts have been made to gain information on the structure of PITN using Raman spectra of electrochemically polymerized samples[22,23] and NMR measurements on model compounds.[20,24] In Ref. 22, Cuff *et al.* reported evidence of the quinonoid ground state of PITN by comparing the calculated frequencies of aromatic (A) and quinonoid (Q) models of PITN (using SQMOFF with a minimum basis set and uniform scaling). The observed experimental frequency shifts upon electrochemical doping were consistent with the transition from a quinonoidlike structure to an aromaticlike structure. In this work a more refined calculation, with a better basis set and with nonuniform scaling has been done. The Raman spectra of PThP have been published by Kastner *et al.*[19] with an analysis that was based on SQMOFF. By bringing together the SQMOFF based vibrational analysis of doped and undoped polythiophene with these two thiophene based polymers we obtained a better understanding of the spectra and structures of conjugated heterocyclic conducting polymers in which there is a competition between two alternative structures.

II. COMPUTATIONAL METHODS

A. Overview of the SQMOFF method

We use the SQMOFF method[9(a)] to calculate the vibrational frequencies and intensities of the polymers. It is a polymer variant of Wilson's GF method,[25] that is based on a quantum mechanically determined force constant matrix and on periodic boundary conditions for an infinite chain.[26,27] The G matrix in Cartesian coordinates is comprised of the inverse atomic masses of the repeat unit. The F matrix is extracted from the force matrix of the middle segment of an oligomer force matrix that was obtained by *ab initio* quantum mechanical calculation that has undergone an empirical scaling process. *Ab initio* methods have been found to be the most reliable in predicting frequencies and relative intensities.[9,10,28–39] In this work we have used the 3-21G and the 3-21G* basis sets.[40] The IR and nonresonant (Placzek-type) Raman intensities of polymers have been calculated using the dipole moment and polarizability derivatives that are calculated from the middle segment of oligomers[40] and then extrapolated to the polymers.[9]

The accurate determination of the F matrix is the crucial point, which proceeds along the following steps:

(1) Properly chosen small molecule (thiophene) is studied, a handful of scaling factors are determined using the experimental vibrational spectra of the monomer. The scaling factors are defined in terms of local vibrational coordinates in a chemically meaningful way, for instance as recommended by Pulay.[35,36] This ensures transferability of the scaling factors and is critical in the success of the technique.

This article is copyrighted as indicated in the article. Reuse of AIP content is subject to the terms at: http://scitation.aip.org/termsconditions. Downloaded to IP: 128.114.34.22 On: Fri, 28 Nov 2014 10:08:48

TABLE I. Definitions off the internal coordinates of thiophene.[a]

No.	Definitions	Descriptions
$S_{1\&2}$	$R(2,4), R(3,5)$	C═C stretch
S_3	$R(4,5)$	C–C stretch
$S_{4\&5}$	$R(1,2), R(1,3)$	C–S stretch
S_{6-9}	$r(2,6), r(3,7), r(4,8), r(5,9)$	C–H stretch
S_{10-13}	$\gamma(6,1,2,4), \gamma(7,1,3,5), \gamma(8,2,4,5), \gamma(9,3,5,4)$	C–H wag
S_{14-17}	$\beta(6,2,1)-\beta(6,2,4)$, $\beta(7,3,1)-\beta(7,3,5)$, $\beta(8,4,2)-\beta(8,4,5)$, $\beta(9,5,3)-\beta(9,5,4)$	C–H bend
S_{18}	$\alpha(2,1,3)+a[\alpha(1,3,5)+\alpha(1,2,4)]+b[\alpha(3,5,4)+\alpha(2,4,5)]$	Ring deformation
S_{19}	$(a-b)[\alpha(1,3,5)+\alpha(1,2,4)] +(1-a)[\alpha(3,5,4)-\alpha(2,4,5)]$	Ring deformation
S_{20}	$b[\tau(2,1,3,5)+\tau(4,2,1,3)]+a[\tau(1,3,5,4)+\tau(5,4,2,1)]+\tau(3,5,4,2)$	Ring torsion
S_{21}	$(a-b)[\tau(5,4,2,1)-\tau(1,3,5,4)]+(1-a)[\tau(4,2,1,3)-\tau(2,1,3,5)]$	Ring torsion

[a]A general scheme is found in Ref. 36. Normalization factors are chosen such that $(\Sigma n_i^2)^{-1/2}=1$, where n_i are the coefficients for each coordinate. $a=\cos 144°=-0.8090$ and $b=\cos 72°=0.3090$. The coordinates are $R(i,j)=C_i$–C_j bond length, $r(i,j)=C_i$–H_j bond length, $\alpha(i,j,k)=C_i$–C_j–C_k angle, $\beta(i,j,k)=C_i$–C_j–H_k angle, $\gamma(i,j,k,l)=H_i$–C_j out of C_j–C_k–C_l plane, $\tau(i,j,k,l)=C_i$–C_j–C_k–C_l torsion.

(2) Intercell scaling factors are obtained from fitting the calculated spectrum of the dimer or trimer with experiment, if those spectra and their accurate assignments are available.

(3a) An oligomer of suitable size is chosen. The unscaled F matrix is obtained from an ab initio calculation using the same basis set as for the monomer and dimer. Scaling is then performed in the same local vibrational coordinates as used for the monomer and dimer. No experimental data from the polymer spectra are used. (Such is **Set** i in Table IV.) A prediction of the polymer spectra follows, based on the assumption of periodicity of the polymer. Sometimes an even better fit can be obtained by further adjusting a limited number of inter-ring scaling factors.

(3b) For highly doped polymers, or many other polymers, no convenient model dimers exist to use in determining the inter-ring scaling factors. In such cases we use the polymer spectrum and determine a small number of scaling factors corresponding to those bonds that change dramatically upon doping.

Convergency properties of the SQMOFF technique with respect to the oligomer size showed—in agreement with earlier convergency studies[9,14]—that the middle unit of a trimer is a reasonable starting point for the SQMOFF calculation. We have also investigated the influence of second neighbor thiophene–thiophene interactions using a pentamer and have found that the various coupling force constants between the central unit and the end unit are practically zero, in agreement with earlier convergency studies.[9,30,31]

B. Choice of basis set and scaling factors

At the ab initio Hartree–Fock HF level vibrational frequencies are usually overestimated[34] primarily because of electron correlation effects. To correct for these systematic errors, Pulay[36,39] proposed to scale the ab initio HF force constants such that

$$F_{i,j}^{\text{scaled}}=(S_iS_j)^{1/2}F_{i,j}^{\text{ab initio}},$$

where S_i's are the scaling factors. In the SQMOFF approach, we adopt a version of Pulay's scaling scheme. We obtain scaling factors from monomers by a least-squares minimization of the rms error $\{\Sigma_i[(\upsilon_{i,\text{expt}}-\upsilon_{i,\text{calcd}})/(N-1)]^2\}^{1/2}$, where υ_{expt} and υ_{calcd} are experimental and calculated frequencies of the monomer, and N is the number of normal modes. The scaling factors obtained with this method are then transferred and used in the polymer calculations.

The definitions of the internal coordinates of thiophene are described in Table I and Fig. 2. The best fit yielded a rms error of 9.9 and 8.4 cm^{-1} for the 3-21G and the 3-21G* basis sets, respectively. However, the error of 9.9 cm^{-1} can be reduced to 8.9 cm^{-1} by introducing a separate scaling factor for the CC/CC coupling force constants (see Table II) such that all CC/CC coupling force constants are uniformly scaled.

Vibrational frequencies and intensities of thiophene obtained with this modified Pulay scaling scheme[35] are listed and compared with experiment[49] in Table III.

All scaling factors used in the undoped PTh calculation are transferred from thiophene except for the inter-ring

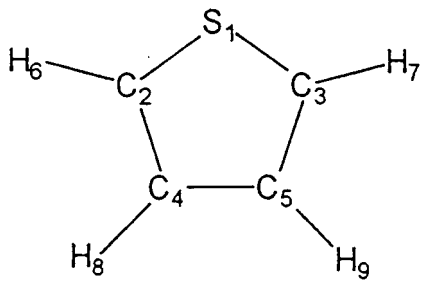

FIG. 2. Atom labels of thiophene. See Table I for the internal coordinate definitions using this numbering.

This article is copyrighted as indicated in the article. Reuse of AIP content is subject to the terms at: http://scitation.aip.org/termsconditions. Downloaded to IP: 128.114.34.22 On: Fri, 28 Nov 2014 10:08:48

TABLE II. Force constants and scaling factors of thiophene.

No.	Int. coord. descriptions	Scaling factors this work (3−21G) Set I[c]	Scaling factors this work (3−21G) Set II[d]	Force constants[a,b] this work Set I[c]	Force constants[a,b] this work Set II[d]	Ref. 11(c)
1&2	C═C stretch	0.7261	0.7274	7.245	7.257	7.141
3	C–C stretch	1.0234	1.0391	5.833	5.923	5.867
4&5	C–S stretch	1.1401	1.1380	4.017	4.009	
6–9	C–H stretch	0.8186	0.8185	5.358	5.357	
10–13	C–H wag	0.6430	0.6430	0.331	0.331	
14–17	C–H in-plane deformation	0.7780	0.7763	0.397	0.396	
18&19	Ring deformation	0.8050	0.8072	1.656	1.660	
				1.426	1.430	
20&21	Ring torsion	0.8234	0.8234	0.429	0.429	
				0.416	0.416	
	CC/CC coupling	$(S_iS_j)^{1/2}$	0.9892			

[a]The units for stretching and bending force constants are mdyn/Å and mdynÅ/rad^2, respectively.
[b]The complete scaled quadratic force matrix is available as supplementary material.
[c]See text, Pulay scaling.
[d]See text, modified Pulay scaling.

modes. Ehrendorfer and Karpfen[10(b)] have solved this problem in their analysis of the spectra of bithiophene by using the same interring CC scaling factors as the intraring ones. As a consequence, their fit for the dimer is not as good as that of thiophene itself. We have chosen a similar route by using for inter-ring scaling factors the value of 0.8000 (Set i).

In the left half of Table IV, the calculated A_g frequencies for PTh are compared to those observed experimentally. The predicted values by Set i for modes 1 and 5 agree well with the experiment. To correct for the overestimation of modes 2 through 4, the C_β–C_β stretching scaling factor is reduced from 1.0391 to 0.8700. This is done manually with an initial step size of 0.05 and then 0.02. The initial unrefined scaling factors constitute Set i, after refinement we obtained Set ii, leading to an excellent agreement with experiment.

TABLE III. Scaled (set II) SCF (3-21G) vibrational frequencies and intensities of thiophene.[a]

Species	Calc freq (cm^{-1})	IR Int (km/mol)	Raman Int (Å^4/amu)	Expt freq[b] (cm^{-1})	Expt Rel Int[c]
In-plane					
A_1	3136	3.11	197	3126	*m*
	3087	1.72	109	3089	*s*
	1413	0.012	34.8	1409	*s*
	1355	7.87	13.8	1360	*w*
	1079	2.21	9.13	1081	*s*
	1029	2.08	16.4	1036	*w*
	827	38.9	15.1	839	*vs*
	610	0.37	8.89	608	*w*
B_2	3131	0.00	2.92	3125	
	3072	5.00	81.6	3086	*s*
	1506	0.82	0.62	1504	*w*
	1253	15.4	1.85	1256	*s*
	1092	2.12	5.79	1083	
	882	3.11	0.20	872	*m*
	763	0.28	5.60	751	*vw*
Out-of-plane					
A_2	899	0.00	4.24	903	
	706	0.00	4.77	688	
	583	0.00	0.45	567	
B_1	865	0.51	0.01	867	
	684	189.0	1.71	712	*s*
	433	0.18	2.22	452	*w*
rms error	8.9[d]				

[a]The $x-z$ plane is the molecular plane; therefore, the A_2 modes are only Raman active.
[b]From Ref. 49.
[c]IR intensity. Notations: *v*=very, *s*=strong, *m*=medium, *w*=weak.
[d]The rms error is defined as $\{\Sigma_i[v_i(\text{calc})-v_i(\text{expt})/(N-1)]^2\}^{1/2}$, where v_i's are the frequencies and N is the number of frequencies. The corresponding rms error based on set I scaling factors is 9.9 cm^{-1}. Scaled 3-21G* frequencies have a rms error of 8.4 cm^{-1}.

C. Modeling of polymers with quinonoidlike structures

In order to ensure a quinonoid structure within an oligomer, we have used terminal CH_2 groups as shown in Fig. 3. Such models will be referred to as the **Q** models, while the single bond capped oligomer is the **A** model. All scaling factors, with the exception of the inter-ring scaling factors, were transferred from thiophene for undoped PTh, from benzene and thiophene for undoped PITN, and from pyrazine and thiophene for undoped PThP. The inter-ring scaling factor for stretching is manually varied to obtain a reasonably

TABLE IV. Comparison between the calculated Raman active A_g mode frequencies of undoped and heavily doped PTh and experimental values.

	Undoped PTh				Heavily doped PTh		
Mode #	Calc (model **A**) Set i[a]	Set ii	Expt Ref. 12	Ref. 13	Calc (Model **Q**)	Expt Ref. 12	Ref. 13
1	1462	1456	1455	1461	1422	1418	1419
2	1390	1352	1365	1369	1352	1350	1356
3	1210	1179		1176	1141	1140	1156
4	1076	1046	1045	1046	1052	1048	1062
5	702	701	700		632	640	

[a]Set i refers to the initial unrefined scaling factors. Set ii consists of a refined intraring C_β–C_β stretching force constant of 5.211 mdyn/Å.

This article is copyrighted as indicated in the article. Reuse of AIP content is subject to the terms at: http://scitation.aip.org/termsconditions. Downloaded to IP: 128.114.34.22 On: Fri, 28 Nov 2014 10:08:48

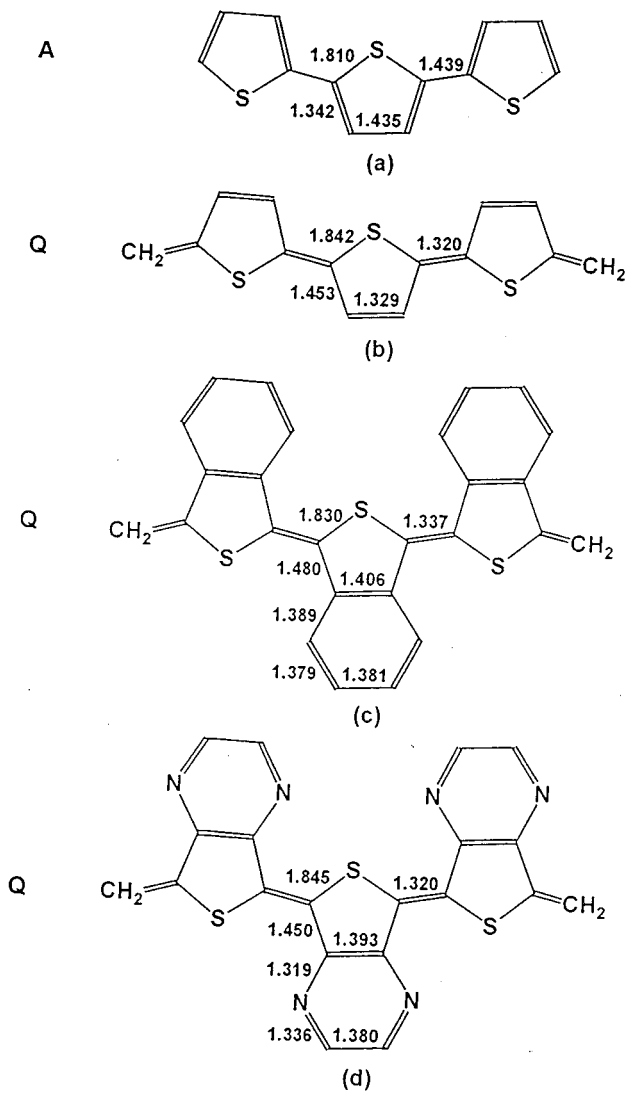

FIG. 3. Trimers used for (a) undoped PTh, (b) heavily doped PTh, (c) undoped PITN, and (d) undoped PThP. Trimers (b)–(d) are capped with CH_2 to ensure a quinonoid (Q) structure. Optimized bond lengths (Å) correspond to the 3–21 G basis set.

good fit with the experimental Raman spectrum. All other inter-ring (torsion, in-plane and out-of-plane bending) scaling factors are set at 0.8000.

For PITN and PThP it was necessary to explore a range of interring CC stretching scaling factors rather than adopting the typical value of 0.8 by varying it in 0.05 or 0.02 steps until a good agreement with the experimental Raman spectrum was obtained, yielding an inter-ring stretching scaling factor of 0.60 for PITN and 0.55 for PThP.

The rationale for modeling the heavily doped PTh polymer with a **Q** model has been described in our earlier paper on highly doped PPP.[9(b)] Therein we concluded that this infinite **Q** chain resembles the average structure of a *heavily* doped PPP polymer. Further, we also found in connection with PPP [Ref. 9(b)] that the Raman intensities are more sensitive to the quinonoid character of the model than to the charge transfer. This conclusion has been also confirmed by Ehrendorfer and Karpfen[10(b)] in their unscaled calculations on charged and neutral oligomers of thiophene. Therefore, the Q model should be useful in simulating the overall average properties of n- and p-doped polymers at the high doping level limit. The scaling of the Q model can not be done by using scaling factors from thiophene because (1) thiophene is aromatic and (2) the Q model itself represents a pure (100%) quinonoid structure. Therefore, we need to fit our model to obtain experimental frequencies by adjusting some selected scaling factors. As a by-product, such a fitting process will yield a measure of the partial quinonoid character of the doped material.

In order to keep the number of adjustable parameters at a minimum, we vary the scaling factors only for the three different CC stretching force constants. This is done manually with an initial step size of 0.05 and then 0.02. All other scaling factors are the same as those used in undoped PTh. At the end of the process, we obtained a force field that produced excellent agreement with the available experimental data, as can be seen from the data in the right half of Table IV, both in terms of the frequency values and the shifts of the frequencies relative to the undoped phase. Overall, the intensity predictions are also consistent with experiment.

III. DETERMINATION OF BOND DISTANCES THROUGH THE APPLICATION OF BADGER'S RULE

The scaled CC stretching force constants can be used to calculate the respective CC bond lengths using Badger's rule.[41,42] Accordingly, $F^{-1/3}=ar+b$, where F is the stretching force constant in mdyn/Å, r is the CC bond length in Å, and a and b are constants. We plotted the scaled CC stretching force constants of a number of small molecules vs experimental bond lengths and obtained a good fit through the relationship $F^{-1/3}=0.746r-0.511$. The small molecules used are ethylene,[43] butadiene,[43] hexatriene,[44] cyclopentene,[45] cyclopentadiene,[46] fluorene,[47] and benzene.[48]

Geometrical data of thiophene obtained using different basis sets are compared with experimental values[50] in Table V. The 3-21G basis set gives larger C–C and C–S bond lengths, and the bond alternation (Δr in Table V) is overestimated by the 3-21G, 3-21G* and 6-31G* basis sets. As a result of the overestimation of the C–C and C–S bond lengths, the corresponding optimized scaling factors become larger than 1.0. While reduction in bond alternation close to the experimental value can be achieved with correlated calculations, such as MP2, the same level of agreement can be achieved with bond distances obtained from Badger's rule. Using the modified Pulay scaling scheme described above, the scaled 3-21G C–C and C═C stretching force constants were determined. Based on Badger's rule, these force constants were estimated to correspond to bond lengths of 1.38 and 1.43 Å (Table V), yielding a bond alternation value of 0.05 Å which is in excellent agreement with the experimental value of 0.053 Å. The above results clearly illustrate that some effects of electron correlation can be corrected with scaling factors. Because this equation is obtained using neu-

This article is copyrighted as indicated in the article. Reuse of AIP content is subject to the terms at: http://scitation.aip.org/termsconditions. Downloaded to IP: 128.114.34.22 On: Fri, 28 Nov 2014 10:08:48

TABLE V. Optimized geometry of thiophene by different techniques as compared to experimental result.

	Bond lengths (Å) Calc (this work)					
Basis set	3-21G	3-21G*	6-31G*	6-31G*/ MP2	3-21G[a] (Badger's rule)	Expt (Ref. 50)
$C1-S2$[b]	1.797	1.722	1.726	1.718		1.714
$C2-C4$	1.335	1.348	1.345	1.376	1.38	1.370
$C4-C5$	1.448	1.438	1.437	1.420	1.43	1.423
Δr[c]	0.113	0.090	0.092	0.044	0.05	0.053
			Bond angles (deg)			
$C2-S1-C3$	89.2	91.4	91.3	92.0		92.2
$S1-C2-C4$	111.7	111.9	111.8	111.6		111.5
$C2-C4-C5$	113.7	113.0	112.5	112.4		112.5

[a]r_{CC}, estimated based on scaled force constants, from the fit $r=(F^{-1/3}+0.511)/0.746$ (Sec. III).
[b]Numbering as in Fig. 2.
[c]$\Delta r = r_{C4-C5} - r_{C2-C4}$.

tral molecules, its extension to heavily doped or charged species may carry an additional error.

IV. ANALYSIS OF VIBRATIONAL SPECTRA

A. Undoped poly(thiophene)

The symmetry of undoped and doped PTh correspond to a line group that is isomorphous with the D_{2h} point group. Their irreducible representations for the vibrations are

$$7A_{1g}+7B_{1g}+3B_{2g}+3B_{3g}+3A_u+3B_{1u}+6B_{2u}+6B_{3u}.$$

The complete set of calculated frequencies of undoped PTh, is listed in Table VI. The agreement with experiment is much better than in the earlier vibrational calculations. Moreover, our calculations are able to produce reasonable IR and nonresonant Raman intensities, which the earlier calculations did not even attempt to do. It is noted that within the refined set (Set ii) one of the calculated A_g frequencies occurs at 1179 cm^{-1}. This value corresponds to a weak peak in all Raman spectra obtained with solid PTh samples. Furukawa *et al.*[11(b)] pointed out that this might be a peak due to a structural distortion and assigned the 1218 cm^{-1} peak as the inter-ring A_g mode. This assignment is in conflict with our finding. In view of this observation, the assignment of this A_g mode has to be re-examined, e.g., by isotope substitution. Both peaks being very weak, intensity argument cannot resolve the assignment.

B. Highly doped poly(thiophene)

The scaling factors and their corresponding force constants of both undoped and doped PTh are listed in Table VII for comparison. As expected from an aromatic to quinonoid transition, the force constant of the inter-ring stretch increases and the force constant of the intraring C_α–C_β decreases. However, there is only a very slight increase in the intraring C_β–C_β stretching force constant.

Using Badger's rule we estimated the various CC bond lengths of undoped and heavily doped PTh from their corresponding scaled force constants. The bond length differences between the two structures are listed as $\Delta r = r^Q - r^A$ in Table VII. These values have the same signs as those calculated by Bredas *et al.*,[14] based on a model of doped and undoped quaterthiophene using STO-3G optimized geometries, but differ in magnitude. The differences cannot be attributed only to the differences in the basis set and the method used. Consequently, electron correlation must play a significant role, as has been discussed in connection with the results on thiophene itself (Table V). However, as expected, the Hartree–Fock (HF) results of this work agree very well with the HF values of Bredas *et al.*,[14] the differences are attributable to the differences in the basis sets used. The values of Δr estimated from force constants reported in Ref. 12 show only a slight elongation of the C_α–C_β bond which is not accompanied by any shortening of the other CC bonds. This does not fit the picture of an aromatic to quinonoid ''transition'' upon doping.

Assuming that a pure aromatic PTh has inter-ring bond length of 1.47 Å (based on Badger's rule, see Table VII) and the corresponding value for the pure quinonoid PTh is 1.32 Å (model **Q**, based on calculated trimer inter-ring bond length), the inter-ring bond length of 1.42 Å, that is consistent with the vibrational analysis, is estimated to have about 33% quinonoid character. This finding is significant in that it establishes the limits of the **Q** model for describing the structure and properties of highly doped PTh. This result is in agreement with our earlier conclusion concerning highly doped PPP [Ref. 9(b)] exhibiting a 30% quinonoid character.

In Table VIII, we describe the potential energy distribution[27] (PED) of each A_g mode in terms of its components in internal coordinates. Some A_g modes are illustrated in Fig. 4 where the calculated Raman spectra of undoped and heavily doped PTh in the 1000–1600 cm^{-1} region are also shown. First, we note that only two A_g modes, peaks *A* and *C*, shift to lower frequencies. These results are in good agreement with experimental data and can be understood from the PED as described in Table VIII. Peak *A* consists of

This article is copyrighted as indicated in the article. Reuse of AIP content is subject to the terms at: http://scitation.aip.org/termsconditions. Downloaded to IP: 128.114.34.22 On: Fri, 28 Nov 2014 10:08:48

TABLE VI. Assignments of experimentally observed peaks of undoped poly(thiophene) based on calculated (set ii) vibrational frequencies and intensities.[a]

	Calc				Expt			
	This work		Ref. 4	Ref. 28	Ref. 12		Ref. 13	
Species	Freq (cm^{-1})	Int	Freq (cm^{-1})	Freq (cm^{-1})	Freq (cm^{-1})	Rel Int	Freq (cm^{-1})	Rel Int
In-plane								
A_g	3086	84.6	3099	3074				
	1456	5159	1530	1549	1455	*vs*	1461	*vs*
	1352	64.3	1386	1358	1365	*vw*	1369	*vw*
	1179	273	1215	1204			1176	*vw*
	1046	548	1057	1083	1045	*s*	1046	*s*
	701	16.8	707	748	700	*w*		
	294	1.44	285	291				
B_{1g}	3072	54.6	3082	3068				
	1548	138	1591	1582	1503	*w*	1498	*w*
	1262	38.4	1289	1274				
	1244	9.54	1250	1191				
	765	2.84	752	733				
	529	1.02	516	524				
	394	0.95	397	402				
B_{2u}	3086	0.01	3099	3076				
	1410	13.1	1459	1420	1476	*w*	1440	*w*
	1256	0.02	1246	1305				
	1046	2.61	1072	1121				
	847	11.9	844	879	836	*w*	836	*w*
	600	0.38	600	604			581	*w*
B_{3u}	3072	22.8	3082	3068				
	1498	31.4	1495	1489	1490	*s*	1490	*s*
	1211	3.78	1199	1212	1230	*vw*		
	923	0.11	917	944				
	770	2.02	758	726	738	*vw*	738	*vw*
	193	0.17	192	195				
Out-of-plane								
B_{2g}	887	55.9	907	893				
	632	12.2	632	642				
	428	0.65	411	393				
B_{3g}	830	0.46	818	793				
	612	3.11	559	612				
	137	0.14	145	137				
A_u	860	0.00	883	793				
	575	0.00	589	581				
	168	0.00	165	154				
B_{1u}	783	68.8	801	772	790	*vs*	786	*vs*
	467	7.49	457	490				
	27	1.81	0	43				

[a]Units for IR (u modes) and Raman (g modes) intensities are km/mol and Å^4/amu, respectively.

a mixture of inter-ring stretching and intraring C_α–C_β stretching components. Upon doping, the inter-ring bond acquires double bond character but the intraring C_α–C_β bond loses double bond character. As a result, there is a net loss of C═C double bond stretching component in this normal mode upon heavy doping. In the case of peak *B*, it is mainly made up of a mixture of C–C, C═C, and C–S stretching components. Upon doping, the C═C stretching component decreases and the C–C increases significantly, resulting in a downward frequency shift. It must be pointed out that it is not very helpful to label either of these modes as the ''inter-ring'' stretching mode. The major components of peaks *B* and *C* are C–H bend and intraring C_β–C_β stretch. As indicated in Table VII, there is only a slight increase in the intraring C_β–C_β stretching force constant upon doping. Therefore, there is very little change in these two vibrational frequencies.

C. Undoped PITN

The line group of PITN is isomorphous to D_{2h} point group, the irreducible representations of the vibrational modes are

$$13A_{1g}+5B_{1g}+13B_{2g}+7B_{3g}+5A_u+12B_{1u}+7b_{2u}+12B_{3u}.$$

The vibrational frequencies and intensities of undoped PITN were calculated using the scaling factors of thiophene and benzene.[30] Since the experimental IR spectrum is unavail-

This article is copyrighted as indicated in the article. Reuse of AIP content is subject to the terms at: http://scitation.aip.org/termsconditions. Downloaded to IP: 128.114.34.22 On: Fri, 28 Nov 2014 10:08:48

TABLE VII. Scaling factors and force constants of undoped and heavily doped polythiophene.

	Undoped PTh			Heavily doped PTh			Δr^f (Å)			
Description	Scaling factors (set ii)	Force constants[a]	Estimated[b] bond length r_i^A (Å)	Scaling factors	Force constants[a]	Estimated[b] bond length r_i^Q (Å)	This work SQMOFF	HF[g]	Ref. 14	Ref. 12[h]
C_β–C_β stretch	0.8700[c]	5.211	1.46(2)	0.5200[e]	5.469	1.45(2)	−0.01	−0.106	−0.074	0.00
C_α–C_β stretch	0.7274	6.989	1.39(2)	0.8000[e]	4.435	1.50(2)	+0.11	+0.111	+0.086	0.03
Inter-ring C–C stretch	0.8000[d]	4.930	1.47(2)	0.5600[e]	6.084	1.42(2)	−0.05	−0.119	−0.118	0.00
C–S stretch	1.1380	3.990		1.1380	3.719					
C–H stretch	0.8185	5.194		0.8185	5.194					
C–H in-plane deformation	0.7763	0.467		0.7763	0.471					
C–H wag	0.6430	0.357		0.6430	0.361					
Ring deformation	0.8072	1.677		0.8072	1.529					
		1.430			1.390					
Ring torsion	0.8234	0.392		0.8234	0.306					
		0.363			0.114					
Inter-ring wag	0.8000[d]	0.540		0.8000[d]	0.465					
Inter-ring bend	0.8000[d]	0.786		0.8000[d]	0.793					
Inter-ring torsion	0.8000[d]	0.002		0.8000[d]	0.108					
CC/CC coupling	0.9892			0.9892						

[a]The units for stretching and bending force constants are mdyn/Å and mdyn Å/rad^2, respectively.
[b]Using Badger's rule.
[c]In set i, this value is 1.0391. See Sec. II B and Table IV for further details.
[d]Since there are no corresponding scaling factors in thiophene, these scaling factors are arbitrarily set at 0.8000. See text for details.
[e]These scaling factors are obtained by fitting calculated frequencies to experimental Raman frequencies of doped polythiophene. See text for details.
[f]$\Delta r_i = r_i^Q - r_i^A$.
[g]Based on data in Fig. 3.
[h]Estimated values based on the force constants reported in Ref. 12.

able, this discussion will deal with Raman active modes (especially the A_g modes) only. The calculated Raman spectrum of PITN, in the 1000–1600 cm^{-1} region, together with displacement vectors are shown in Fig. 5. The potential energy distributions (PED) of the A_g modes are described in Table IX. Compared to the same region of heavily doped PTh (which is quinonoid), there are two additional peaks in the calculated undoped but quinonoidlike PITN Raman spectrum. The 1504 cm^{-1} and 1225 cm^{-1} modes are unique to PITN and have no corresponding bands in either benzene or heavily doped PTh. The others resemble those of benzene or polythiophene. The mode at 1592 cm^{-1} can be attributed to benzene ring stretching mode. The 1433 cm^{-1} mode can be viewed as modified peak *A* of heavily doped PTh (1422 cm^{-1}). This slight increase in frequency is indicative of a small influence due to the benzene substructure. The 1334 cm^{-1} peak has its origin in benzene (1350 cm^{-1}). The 1190 cm^{-1} peak can be attributed to the C–H bending mode of the benzene substructure. It is noted that the 1504 and 1433 cm^{-1} modes have significant inter-ring stretching component

TABLE VIII. Calculated Raman frequencies (cm^{-1}), Raman activities Å/amu, and PED (%) of the A_g modes of undoped and heavily doped polythiophene. Experimental frequencies are listed for comparison.

Undoped PTh					Heavily doped PTh			
Mode label	Expt[a] Freq	Calc Freq	Activity	PED[b]	Expt[a] Freq	Calc Freq	Activity	PED[b]
	⋯	3086	84.6	99 C–H stretch	⋯	3087	86.8	99 C–H stretch
A	1455	1456	5159	54 C═C stretch 20 C–C_{ext} stretch 14 ring deform	1418	1421	20702	45 C═C_{ext} stretch 16 C–C stretch 19 ring deform
B	1365	1352	64.3	29 C–C stretch 47 C–H bend 7 C–S stretch 6 C═C stretch	1350	1352	860	46 C═C stretch 48 C–H bend
C	1176[c]	1179	272.8	28 C═C stretch 26 C–C stretch 23 C–S stretch 11 C–C_{ext} stretch	1140	1141	10767	20 C═C stretch 50 C–C stretch 18 C–S stretch
D	1045	1046	548.2	38 C–C stretch 46 C–H bend	1048	1052	1665	28 C═C stretch 49 C–H bend
E	700	701	16.78	42 C–S stretch 10 C═C stretch 35 ring deform	640	632	963	34 C–S stretch 36 C–C stretch 25 ring deform
	⋯	294	1.44	36 C–S stretch 16 C═C stretch 21 ring deform 16 C–C_{ext} bend	⋯	307	18.45	41 C–S stretch 15 C–C stretch 18 ring deform 14 C═C_{ext} bend

[a]From Ref. 12. Laser excitation wavelength is 647.1 nm for both undoped and heavily doped PTh.
[b]Only the main contributions are given.
[c]From Ref. 13.

This article is copyrighted as indicated in the article. Reuse of AIP content is subject to the terms at: http://scitation.aip.org/termsconditions. Downloaded to IP: 128.114.34.22 On: Fri, 28 Nov 2014 10:08:48

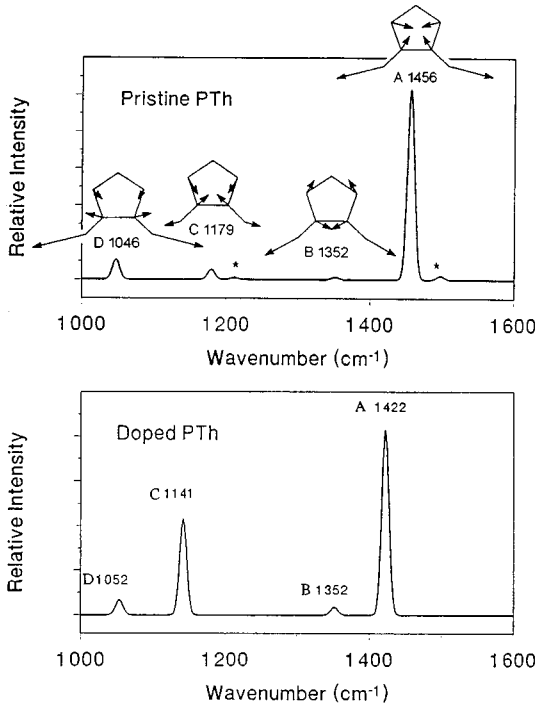

FIG. 4. Calculated Raman spectrum of undoped PTh (top) and heavily doped PTh (bottom) in the 1000–1600 cm^{-1} region. Displacement vectors of the A_g modes are also shown. Asterisks mark the B_{3g} modes of undoped PTh which are observed experimentally.

(see Table IX). In summary, the two peaks at 1504 and 1225 cm^{-1} can be considered as the ''fingerprint'' of PITN. It is also important to note that the Raman spectrum of undoped PITN is not simply a composite of heavily doped PTh and benzene spectra.

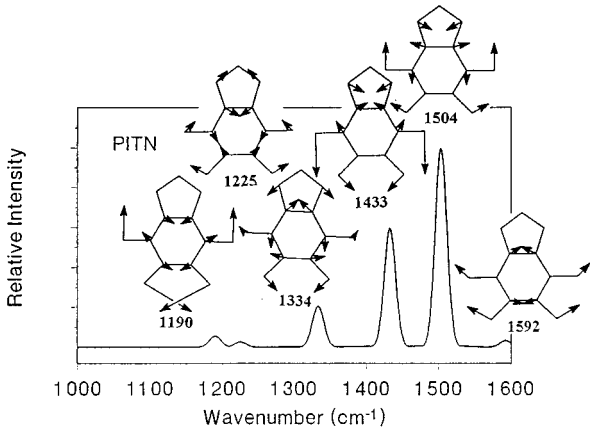

FIG. 5. Calculated Raman spectrum of undoped PITN in the 1000–1600 cm^{-1} region. Displacement vectors of the A_g modes are also shown.

The scaling factors and corresponding force constants of undoped PITN are listed in Table X. Of particular interest is the inter-ring stretching force constant of 6.293 mdyn/Å, which is very close to that of heavily doped PTh, corresponding to about 33% quinonoid character. This observation provides further evidence that the average ground state of PITN is about 30% quinonoid. The inter-ring bond length of PITN is estimated by Badger's rule to be 1.41 Å and is illustrated together with other estimated CC bond lengths based on Badger's rule in Fig. 6.

D. Undoped PThP

The vibrational frequencies and intensities of PThP were calculated in the same way as for PITN. The D_{2h} irreducible representations of the vibrational modes are

TABLE IX. Calculated Raman frequencies (cm^{-1}), Raman activities ($Å^4$/amu), and PED (%) of the A_g modes of undoped PITN. Experimental frequencies are listed for comparison.

Mode #	Expt[a] Freq	Calc Freq	Raman Activity	PED[b]
1	⋯	3170	88.81	98% C–H stretch
2	⋯	3078	245.1	98% C–H stretch
3	1595	1592	158.4	69% C–C (Bz) stretch 16% C–H bend 10% Bz ring deform
4	1490	1504	4981	16% C–C (Bz) stretch 11% C═C_{ext} stretch 31% C–C (Th) stretch 31% C–H bend
5	1445	1433	2993	10% C–C (Bz) stretch 22% C═C_{ext} stretch 23% C–C (Th) stretch 33% C–H bend
6	1310	1334	1028	45% C–C (Bz) stretch 9% (C═C)$_{ext}$ bend
7	1215	1225	131.8	24% C–C (Bz) stretch 34% C–C (Th) stretch 18% C–S stretch 16% C═C_{ext} bend
8	1167	1190	276.8	14% C–C (Bz) stretch 83% C–H bend
9	-	1093	13.08	55% C–C (Bz) stretch 27% C–H bend 12% C═C_{ext} bend
10	985	1025	139.6	63% C–C (Bz) stretch 12% C–S stretch 23% C═C_{ext} bend
11	665	671	5.53	10% C–C (Bz) stretch 78% Bz ring deform
12	450	456	48.01	9% C–C (Th) stretch 35% C–S stretch 26% Th ring deform. 22% Bz ring deform
13	240	277	5.41	12% C–C (Bz) stretch 41% C–C (Th) stretch 23% C═C_{ext} bend

[a]From Ref. 22.
[b]Only the main contributions are given. Notation: Bz=benzene, Th=Thiophene.

This article is copyrighted as indicated in the article. Reuse of AIP content is subject to the terms at: http://scitation.aip.org/termsconditions. Downloaded to IP: 128.114.34.22 On: Fri, 28 Nov 2014 10:08:48

TABLE X. Scaling factors and force constants PITN.

Int. coord. descriptions	Scaling factors	Force constants[a]
C–C (Bz) stretch	0.8725	See Fig. 6
C–C (Th) stretch	1.0234	See Fig. 6
Inter-ring C═C_{ext} stretch	0.6000	6.293
C–S stretch	1.1401	4.206
C–H stretch	0.8279	5.517, 5.168
C–H wag	0.7134	0.393, 0.433
C–H in-plane deformation	0.7666	0.555, 0.501
Th ring deformation	0.8050	1.742
		2.117
Th ring torsion	0.8234	0.103
		0.004
Bz ring deformation	0.7438	1.576
		1.757
		1.498
Bz ring torsion	0.7367	0.259
		0.248
		0.224
Inter-ring torsion	0.8000	0.429
Inter-ring bend	0.8000	3.023
Inter-ring wag	0.8000	0.461
CC/CC coupling	0.6912	

[a]The units for stretching and bending force constants are mdyn/Å and mdyn Å/rad^2, respectively. Notations: Bz=Benzene, Th=Thiophene.

TABLE XI. Scaling factors and force constants of PThP.

Int. coord. descriptions	Scaling factors	Force constants[a]
C–N stretch	0.8736	See Fig. 6
C–C (Pz) stretch	0.8565	See Fig. 6
C–C (Th) stretch	1.0234	See Fig. 6
Inter-ring C═C_{ext} stretch	0.5500	6.119
C–S stretch	1.1401	3.948
C–H stretch	0.7982	5.092
C–H wag	0.7147	0.445
C–H in-plane deformation	0.8106	0.546
Th ring deformation	0.7423	1.617
		1.749
Th ring torsion	0.7046	0.195
		0.185
Pz ring deformation	0.7423	1.401
		1.655
		1.238
Pz ring torsion	0.7046	0.230
		0.242
		0.237
Inter-ring torsion	0.8000	0.483
Inter-ring bend	0.8000	1.310
Inter-ring wag	0.8000	0.540
CC/CC coupling	0.6013	

[a]The units for stretching and bending force constants are mdyn/Å and mdyn Å/rad^2, respectively. Notations: Pz=Pyrazine, Th=Thiophene.

$$11A_{1g}+5B_{1g}+11B_{2g}+5B_{3g}+5A_u+10B_{1u}+5B_{2u}+10B_{3u}.$$

The complete set of scaling factors and corresponding force constants are listed in Table XI. As with PITN, the inter-ring force constant of PThP (6.148 mdyn/Å) is very close to that of heavily doped PTh. The estimated inter-ring bond length, based on Badger's rule is 1.42 Å, indicating that the average structure is about 30% quinonoidlike. The scaled CC and CS stretching force constants are summarized in Fig. 6 for an easy comparison.

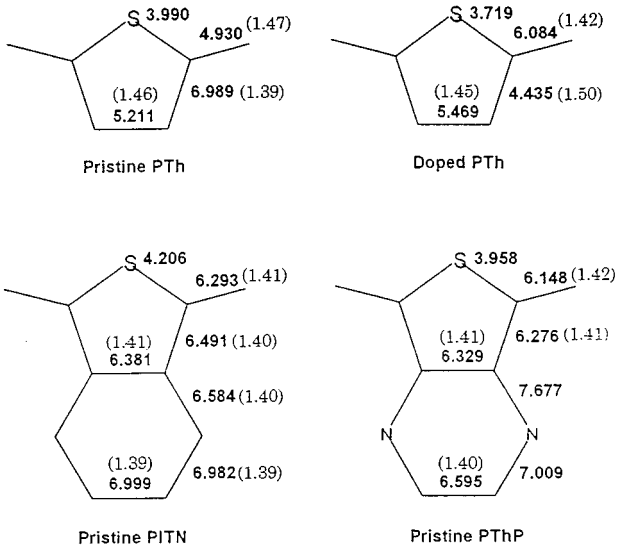

FIG. 6. Scaled CC and CS stretching force constants of (top): undoped and heavily doped PTh, (bottom): undoped PITN and PThP. Numbers in parentheses are estimated bond lengths based on the relationship $r=(F^{-1/3}+0.511)/0.746$, where r is in Å and F is in mdyn/Å.

The calculated Raman spectrum of PThP depicting the A_g modes and their respective Cartesian displacement vectors are shown in Fig. 7. The PED descriptions are listed in Table XII. The 1572 cm^{-1} peak can be attributed to the pyrazine substructure. Besides this mode, the 1127 and 1168 cm^{-1} modes also consist of largely pyrazine ring stretching. The 1535, 1360, and 1299 cm^{-1} modes are unique to PThP. The PED of mode #3 (1535 cm^{-1}) is similar to peak A of undoped and heavily doped PTh but with a smaller C═C stretching contribution. Despite the lower C═C stretching component, it has a higher frequency. This appears to be due to the influence of pyrazine substructure.

V. RAMAN INTENSITY OF UNDOPED AND HEAVILY DOPED PTh

The intensity ratios of the A_g modes of undoped and PTh as calculated with the SQMOFF method are compared to experimental values[12] in Table XIII. The agreement is remarkably good. Because the ground state to excited state transition of PTh involves an aromatic to quinonoid transition [structural changes along the lines illustrated in Figs. 1(a) and 1(b)], one can define a totally symmetric stretching mode. $я_1$ mode,[51] to be proportional to $2\delta r_{C\alpha C\beta}-\delta r_{C\beta C\beta}-\delta r_{\text{inter-ring}}$.

Based on this $я_1$ mode definition, we calculated the intensity ratios, of each A_g mode listed in Table XIII using the effective conjugation coordinates (ECC) theory of Zerbi *et al.*[51–53] Accordingly, the intensity ratio is given by $I_j/I_k=|L_{я1,i}|^2/|L_{я1,k}|^2$, where I_j and I_k are the intensities of jth

This article is copyrighted as indicated in the article. Reuse of AIP content is subject to the terms at: http://scitation.aip.org/termsconditions. Downloaded to IP: 128.114.34.22 On: Fri, 28 Nov 2014 10:08:48

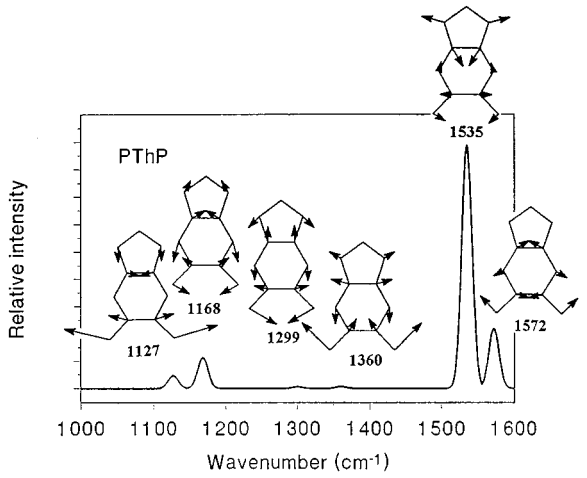

FIG. 7. Calculated Raman spectrum of undoped PThP in the 1000–1600 cm^{-1} region. Displacement vectors of the A_g modes are also shown.

and kth modes, respectively. This follows from the main assumption of this theory which states that all nonzero Raman intensities are originating from a single $я$ mode that is most strongly coupled to the change of geometry upon π to π^* excitation, i.e., the $я_1$ mode. Let $я=\mathbf{L}_я\mathbf{Q}$ and $\mathbf{X}=\mathbf{L}_x\mathbf{Q}=\mathbf{B}^{-1}$ $я$, where $я$ is an internal coordinates matrix which includes the $я_1$ vector, $\mathbf{X}$ is the eigenvector matrix in Cartesian coordinates, $\mathbf{Q}$ is the normal mode matrix, $\mathbf{L}_я$, $\mathbf{L}_x$, and $\mathbf{B}^{-1}$ are transformation matrices. We can then write $\mathbf{L}_я=\mathbf{B}\mathbf{L}_x$. Thus, $L_{я1,j}=B_{я1}L_{x,j}$. The row vector $B_{я1}$ is determined by the definition of the $я_1$ internal coordinate and the eigenvectors L_{xj} are determined from the polymer vibrational modes calculations. From Table XIII, it can be seen that the calculated ECC intensity ratios are very similar to those obtained by the SQMOFF method. This agreement shows that the transition from ground state to the excited state indeed involves a change from an aromatic to a quinonoid structure and that there is a strong electron–phonon coupling in this polymer.

TABLE XIII. Comparison of intensity ratios of the five A_g modes of undoped and doped PTh as predicted by the SQMOFF method and the ECC theory with experimental values.

Undoped PTh				Doped PTh			
Frequency (cm^{-1})	Intensity ratio SQMOFF	Ecc	Expt[a]	Frequency (cm^{-1})	Intensity ratio SQMOFF	ECC	Expt[a]
1456	100	100	100	1422	100	100	100
1352	1.25	2.87	3.1	1352	4.2	11	4
1179	5.29	7.07	4.6	1141	52	68	12
1046	10.6	12.7	15	1052	8.0	7.9	17
701	0.0325	0.0412	4.6	632	4.6	5.9	8

[a]Estimated from Ref. 12. Because of bad baseline, only rough estimates can be made.

Based on our present and previous results[10,30,31] (undoped, heavily doped, and planarized PPP), we observe that the ECC or $я$ mode theory is able to predict the relative Raman intensities correctly if the $я_1$ mode is correctly defined. This is quite remarkable, considering the simplicity of this theory. In the case of straight chain and simple ring polymers, the application of the ECC theory is straightforward. However, when the definition of the $я_1$ mode is not obvious (e.g., planarized PPP which has a methylene bridge between two phenyl rings in a repeat unit or PITN), the application of the ECC theory may be difficult.

VI. CONCLUSIONS

The CC bond lengths of four thiophene based polymers-undoped and heavily doped PTh, undoped PITN, and PThP

TABLE XII. Calculated Raman frequencies (cm^{-1}), Raman activities ($Å^4$/amu), and PED (%) of the A_g modes of undoped PThP. Experimental frequencies are listed for comparison.

Mode #	Expt.[a] Freq	Calc Freq	Raman activity	PED[b]
1	⋯	3060	269.5	99% C–H stretch
2	1562	1572	399.1	28% C–N stretch 33% C–C (Pz) stretch 10% C–C (Th) stretch 16% C–H bend.
3	1520	1535	8875	7% C–N stretch 20% C═C_{ext} stretch 55% C–C (Th) stretch 10% Th ring deform.
4	1360	1360	70.19	15% C–N stretch 19% C–C (Pz) stretch 15% C–C (Th) stretch 42% C–H bend.
5	1296	1299	61.46	20% C–N stretch 13% C═C_{ext} stretch 19% C–C (Th) stretch 16% C–S stretch 12% C–H stretch
6	1212	1168	1131	66% C–N stretch 12% C–C (Pz) stretch
7	1125	1127	462.4	54% C–C (Pz) stretch 17% C–H bend.
8	⋯	1032	37.38	44% C–N stretch 18% C–C (Pz) stretch 15% C–S stretch 14% C═C_{ext}-C bend.
9	⋯	646	14.52	12% C–C (Pz) stretch 65% Pz ring deform.
10	⋯	464	89.03	12% C–C (Th) stretch 39% C–S (Th) stretch 25% (Th) ring deform.
11	⋯	241	2.83	11% C–C (Pz) stretch 33% C–C (Th) stretch 13% C–S stretch 30% C═C_{ext}-C bend.

[a]From Ref. 19. The sample used in the experiment was poly(2,3-methyl[3,4-*b*]pyrazine).
[b]Only the main contributions are given. Notation: Pz=Pyrazine, Th=Thiophene.

This article is copyrighted as indicated in the article. Reuse of AIP content is subject to the terms at: http://scitation.aip.org/termsconditions. Downloaded to IP: 128.114.34.22 On: Fri, 28 Nov 2014 10:08:48

polymers were reported for the first time. We concluded that upon doping, the PTh backbone CC bond lengths changed by -0.01, 0.11 -0.05 Å for the C_β–C_β, C_α–C_β, and inter-ring bonds, respectively. This is significantly different from Hartree–Fock predictions and is attributed to the effects of electron correlation. Further, we also estimated that heavily doped PTh has about 33% quinonoid character. The estimated average inter-ring bond lengths of both undoped PITN and PThP show about 30% quinonoid characteristics similar to that of heavily doped PTh. Compared to the repeat unit of PTh, the thiophene ring substructure in PITN and PThP repeat units are significantly modified by the fusion of another ring.

We also presented an analysis of the Raman spectrum-structure relationship of these four polymers. Our results on undoped PTh show that the peak at 1218 cm^{-1} may not be an A_g mode as previously reported. We explained the frequency differences between undoped and heavily doped PTh in terms of the structural changes from the aromatic (A) to quinonoid (Q) form upon doping. The downshift of the ''inter-ring'' stretching frequencies has been attributed to the decrease in the C═C double bond stretching component in these normal modes. Consequently, there is a net decrease in the C═C stretching component in the ''inter-ring'' normal modes of the heavily doped PTh. While some of the A_g modes can be traced back to the thiophene and benzene or pyrazine substructures, a few modes can be identified to uniquely characterize the fused rings and can therefore act as the ''fingerprint'' peaks.

Supplementary material. The complete set of scaled force matrices of thiophene and pyrazine are available from the authors. (Ph.D. thesis of Lilee Cuff, Georgetown University, 1995.)

ACKNOWLEDGMENTS

This work has been supported by grants from the NSF (#DMR-91-15548) and the NSF Pittsburgh Supercomputer Center (#DMR-920006P).

[1] G. L. Baker, in *Electronic and Photonic Applications of Polymers*, ACS Adv. in Chemistry Series 210, edited by M. J. Bowden and S. R. Turner (American Chemical Society, Washington, D.C., 1988), p. 271.
[2] C. Yong, and R. Renyuan, Solid State Commun. **54**, 211 (1985).
[3] (a) P. N. Prasad, J. Swiatkiewicz, and J. Pfleger, Mol. Cryst. Liquid Cryst. **160**, 53 (1988); (b) T. Sugiyama, T. Wada, and H. Sasabe, Synth. Met. **28**, C323 (1989).
[4] J. Roncali, Chem. Rev. **92**, 711 (1992).
[5] F. Wudl, M. Kobayashi, and A. J. Heeger, J. Org. Chem. **36**, 3382 (1984).
[6] (a) M. Pomerantz, B. Chaloner-Gill, L. O. Harding, J. J. Tseng, and W. J. Pomerantz, J. Chem. Soc. Chem. Commun. **1992**, 1672 (b) M. Kobayashi, N. Colaneri, M. Boysel, F. Wudl, and A. J. Heeger, J. Chem. Phys. **82**, 5717 (1985).
[7] (a) Y. S. Lee and M. Kertesz, J. Chem. Phys. **88**, 2609 (1988); (b) Int. J. Quantum Chem. Quantum Chem. Symp. **21**, 163 (1987).
[8] Y. Ikenoue, F. Wudl, and A. J. Heeger, Synth. Met. **40**, 1 (1991).
[9] (a) C. X. Cui and M. Kertesz, J. Chem. Phys. **93**, 5257 (1990); (b) L. Cuff, C. X. Cui, and M. Kertesz, J. Am. Chem. Soc. **116**, 9269 (1994).
[10] (a) Ch. Ehrendorfer and A. Karpfen, J. Phys. Chem. **99**, 5341 (1995); (b) Vibrational Spectrosc. **8**, 293 (1995).
[11] (a) M. Akimoto, Y. Furukawa, H. Takeuchi, and I. Harada, Synth. Met. **15**, 353 (1986); (b) Y. Furukawa, M. Akimoto, and I. Harada, *ibid.* **18**, 151 (1987); (c) M. Kofranek, T. Kovar, H. Lischka, and A. Karpfen, J. Mol. Struct. Theochem **259**, 181 (1992); (d) J. T. Lopez Navarrete and G. Zerbi, J. Chem. Phys. **94**, 965 (1991); (e) J. L. Sauvajol, D. Chenouni, J. P. Lere-Porte, C. Chorro, B. Moukala, and J. Petrissans, Synth. Met. **38**, 1 (1990); (f) Z. Vardeny, E. Ehrenfreund, O. Brafman, A. J. Heeger, and F. Wudl, *ibid.* **18**, 183 (1987).
[12] G. Louarn, J. Y. Mevellec, J. P. Buisson, and S. Lefrant, J. Chim. Phys. **89**, 987 (1992).
[13] Y. Furukawa, N. Yokonuma, M. Tasumi, M. Kuroda, and J. Nakayama, Mol. Cryst. Liquid Cryst. **256**, 113 (1994).
[14] J. L. Bredas, B. Themans, J. G. Fripiat, J. M. Andre, and R. R. Chance, Phys. Rev. B **29**, 6761 (1984).
[15] A. Karpfen and M. Kertesz, J. Phys. Chem. **95**, 7680 (1991).
[16] M. Kertesz, Synth. Met. **69**, 641 (1995).
[17] J. Kurti, P. R. Surjan, and M. Kertesz, J. Am. Chem. Soc. **113**, 9865 (1991).
[18] K. Nayak and D. S. Marynick, Macromolecules **73**, 2237 (1990).
[19] J. Kastner, H. Kuzmany, D. Vegh, M. Landl, L. Cuff, and M. Kertesz, Macromolecules **28**, 2922 (1995).
[20] I. Hoogmartens, P. Adriensens, D. Vanderzande, J. Gelan, C. Quattrocchi, R. Lazzaroni, and J. L. Bredas, Macromolecules **25**, 7347 (1992).
[21] J. Kurti and P. R. Surjan, J. Chem. Phys. **92**, 3247 (1990).
[22] L. Cuff, M. Kertesz, J. Geisselbrecht, J. Kurti, and H. Kuzmany, Synth. Met. **55**, 564 (1993).
[23] E. Faulques, W. Wallnofer, and H. Kuzmany, J. Chem. Phys. **90**, 7585 (1989).
[24] I. Hoogmartens, D. Vanderzande, and H. Martens, Synth. Met. **14/1–2**, 513 (1991).
[25] E. B. Wilson, Jr., J. C. Decius, and P. C. Cross, *Molecular Vibrations* (McGraw–Hill, New York, 1995).
[26] H. Tadokoro, *Structure of Crystalline Polymers* (Wiley, New York, 1979).
[27] See, for example, P. C. Painter, M. M. Coleman, and J. L. Koenig, *The Theory of Vibrational Spectroscopy and its Applications to Polymeric Materials* (Wiley, New York, 1982).
[28] F. J. Ramirez, V. Hernandez, and J. T. Lopez Navarrete, J. Comput. Chem. **15**, 405 (1994).
[29] C. W. Bock, Y. N. Panchenko, and V. I. Pupyshev, J. Comput. Chem. **11**, 623 (1990).
[30] L. Cuff and M. Kertesz, Macromolecules **27**, 762 (1994).
[31] L. Cuff and M. Kertesz, J. Phys. Chem. **98**, 12 223 (1994).
[32] C. X. Cui, M. Kertesz, and H. Eckhardt, Synth. Met. **41–43**, 3491 (1991).
[33] M. Kofranek, H. Lischka, and A. Karpfen, J. Chem. Phys. **96**, 982 (1992).
[34] J. A. Pople, H. B. Schlegel, R. Krishnan, D. J. Defrees, J. S. Binkley, M. J. Frisch, R. A. White, R. F. Hout, and W. J. Hehre, Int. J. Quantum Chem. Quantum Chem. Symp. **15**, 267 (1981).
[35] P. Pulay, G. Fogarasi, and J. E. Boggs, J. Chem. Phys. **74**, 3999 (1981).
[36] G. Fogarasi and P. Pulay, *Vibrational Spectra and Structure*, edited by J. R. Durig (Elsevier, Amsterdam, 1985), Vol. 14, pp. 125–219.
[37] Ch. Ehrendorfer and A. Karpfen, J. Phys. Chem. **99**, 10 196 (1995).
[38] M. Kofranek, T. Kovar, A. Karpfen, and H. Lishka, J. Chem. Phys. **96**, 4464 (1992).
[39] P. Pulay, G. Fogarasi, F. Pang, and J. E. Boggs, J. Am. Chem. Soc. **101**, 2550 (1979).
[40] (a) M. J. Frisch, M. Head-Gordon, G. W. Trucks, J. B. Foresman, H. B. Schlegel, K. Raghavachari, M. A. Robb, J. S. Binkley, C. Gonzalez, D. J. Defrees, D. J. Fox, R. A. Whiteside, R. Seeger, C. S. Melius, J. Baker, R. L. Martin, L. R. Kahn, J. J. P. Stewart, S. Topiol, and J. Pople, GAUSSIAN 90, Gaussian Inc., Pittsburgh, Pennsylvania, 1990; (b) M. J. Frisch, M. Head-Gordon, G. W. Trucks, P. M. Gill, M. W. Wong, J. B. Foresman, B. G. Johnson, H. B. Schlegel, M. A. Robb, E. S. Replogle, R. Gomperts, J. L. Andres, K. Raghavachari, J. S. Binkley, C. Gonzalez, R. L. Martin, D. J. Fox, D. J. Defrees, J. Baker, J. J. P. Stewart, and J. Pople, GAUSSIAN 92, Gaussian Inc., Pittsburgh, Pennsylvania, 1992.
[41] R. M. Badger, J. Chem. Phys. **2**, 128 (1934).
[42] R. M. Badger, J. Chem. Phys. **3**, 193 (1935).
[43] P. Pulay, G. Fogarasi, J. E. Boggs, and A. Vargha, J. Am. Chem. Soc. **105**, 7037 (1983).
[44] G. Fogarasi, P. G. Szalay, P. P. Liescheski, J. E. Boggs, and P. Pulay, J. Mol. Struct. **151**, 341 (1987).
[45] W. D. Allen, A. G. Csaszar, and D. A. Horner, J. Am. Chem. Soc. **114**, 6834 (1992).

This article is copyrighted as indicated in the article. Reuse of AIP content is subject to the terms at: http://scitation.aip.org/termsconditions. Downloaded to IP: 128.114.34.22 On: Fri, 28 Nov 2014 10:08:48

[46] D. Damiani, L. Ferretti, and E. Gallinella, Chem. Phys. Lett. **37**, 265 (1976).
[47] V. K. Belsky, V. E. Zavodnik, and V. M. Vozzhennikov, Acta Crystallogr. C **40**, 1210 (1984).
[48] A. Langseth and P. B. Stoicheff, Can. J. Phys. **34**, 350 (1956).
[49] J. M. Orza, M. Rico, and F. J. Biarge, J. Mol. Spectrosc. **19**, 188 (1966).
[50] B. Bak, D. Christensen, L. Hansen-Nygaard, and J. Rastrup-Andersen, J. Mol. Spectrosc. **7**, 58 (1961).
[51] G. Zerbi, M. Gussoni, and C. Castiglioni, in *Conjugated Polymers*, edited by J. L. Bredas and R. Silbey (Kluwer, Netherlands, 1991), p. 435.
[52] G. Zerbi and B. Chierichetti, J. Chem. Phys. **94**, 4637 (1991).
[53] C. Castiglioni, M. Del Zoppo, and G. Zerbi, J. Raman Spectrosc. **24**, 485 (1993).

This article is copyrighted as indicated in the article. Reuse of AIP content is subject to the terms at: http://scitation.aip.org/termsconditions. Downloaded to IP: 128.114.34.22 On: Fri, 28 Nov 2014 10:08:48